Fourier Transform Infrared Study of the Effect of Different Cations on Bacteriorhodopsin Protein Thermal Stability

Colin D. Heyes, Jianping Wang, Laurie S. Sanii, and Mostafa A. El-Sayed
Laser Dynamics Lab, School of Chemistry and Biochemistry, Georgia Institute of Technology, Atlanta, Georgia 30332

ABSTRACT The effect of divalent ion binding to deionized bacteriorhodopsin (dI-bR) on the thermal transitions of the protein secondary structure have been studied by using temperature-dependent Fourier transform infrared (FT-IR) spectroscopy. The native metal ions in bR, Ca^{2+}, and Mg^{2+}, which we studied previously, are compared with Mn^{2+}, Hg^{2+}, and a large, synthesized divalent organic cation, $((Et)_3N)_2Bu^{2+}$. It was found that in all cases of ion regeneration, there is a pre-melting, reversible conformational transition in which the amide frequency shifts from 1665 to 1652 cm^{-1}. This always occurs at ~80°C, independent of which cation is used for the regeneration. The irreversible thermal transition (melting), monitored by the appearance of the band at 1623 cm^{-1}, is found to occur at a lower temperature than that for the native bR but higher than that for acid blue bR in all cases. However, the temperature for this transition is dependent on the identity of the cation. Furthermore, it is shown that the mechanism of melting of the organic cation regenerated bR is different than for the metal cations, suggesting a difference in the type of binding to the protein (either to different sites or different binding to the same site). These results are used to propose specific direct binding mechanisms of the ions to the protein of deionized bR.

INTRODUCTION

Bacteriorhodopsin (bR) is a 26-kDa protein found in the purple membrane of *Halobacterium salinarum*. The protein binds a retinal chromophore to the Lys216 residue, which absorbs visible light and isomerizes from the all-*trans* to 13-*cis* form. The energy stored at this point drives a photocycle in which a proton is translocated unidirectionally across the membrane. The pH gradient formed allows the bacterium to drive ATP synthesis and hence its metabolism (for reviews see Stoeckenius et al., 1979; Mathies et al., 1991; Ebrey, 1993; Lanyi, 1995). This photosynthesis is the simplest in nature and provides a good model to study such systems as well as being technologically promising for a number of biomolecular opto-electronic applications (Birge et al., 1999; Hampp, 2000).

One of the major unresolved issues of the structure-function relationship of bR is the exact location of bound cations. It has been found that well washed native bR contains ~1 mol of Ca^{2+} and 4 mol of Mg^{2+} to 1 mol of bR (Chang et al., 1985), and that removal of ~75% of the endogenous natural lipids removes most but not all the cations (Griffiths et al., 1996b). Upon removal of the ions by deionization or acidification, the λ_{max} of bR shifts from 568 nm to 603 nm (purple to blue) (Kimura et al., 1984; Mowery et al., 1979), and the proton pumping no longer functions as shown by the fact that the M intermediate is not formed (Chang et al., 1985; Chronister et al., 1986).

Over the past two decades, many experiments have been performed to investigate the effects of adding a number of cations to bR in which the metal ions have been removed by strong acid, chelator, or ion exchange. These experiments have looked at the effect on various function parameters such as kinetics, mechanism, and efficiency of the photocycle (Chang et al., 1985; Chronister et al., 1986; El-Sayed et al., 1995; Drachev et al., 1988) and on structure parameters such as absorption and emission spectra (Jang et al., 1988), diffraction patterns (Hiraki et al., 1981; Heyn et al., 1989; Griffiths et al., 1996a), and thermal stability (Kresheck et al., 1990; Brouillette et al., 1987; Cladera et al., 1988). The recently obtained high-resolution x-ray diffraction data to 1.55 Å did not give an answer as to the location of these cations (Leuke et al., 1999).

Two high-affinity sites were found for Ca^{2+} to bind to deionized bR as well as four to six lower-affinity sites (Zhang et al., 1992), and removal of retinal removes one of the strongly bound cations (Yang and El-Sayed, 1995). A number of groups have suggested that there is at least one specific internal binding site close to retinal and has binding constants dependent on the cation (Jonas and Ebrey, 1991; Ariki and Lanyi, 1986; Zhang et al., 1992). However, a second train of reasoning suggested that all the metals bind only to the lipids of the membrane surface, and the Guoy-Chapman theory explains the shift in the color of the retinal chromophore upon binding by mediation of the surface pH (Szundi and Stoeckenius, 1987, 1988, 1989; Varo et al., 1999).

Jackson and Sturtevant (1978) first showed the presence of two thermal transitions in bR in the range 20–100°C using calorimetry. They found a small, reversible transition at ~80°C and a larger irreversible transition at 97°C. The irreversible transition has been attributed to denaturation of at least part of the protein helices as well as monomerization of the trimer structure (Jackson and Sturtevant, 1978; Hiraki

Submitted August 8, 2001, and accepted for publication October 19, 2001.

J. Wang's present address: Department of Chemistry, University of Pennsylvania, Philadelphia, PA 19104-3803.

Address reprint requests to Dr. Mostafa A. El-Sayed, School of Chemistry and Biochemistry, Georgia Institute of Technology, Atlanta, GA 30332-0400. Tel.: 404-894-0292; Fax: 404-894-0294; E-mail: mostafa.el-sayed@chemistry.gatech.edu.

0006-3495/02/03/1598/09 $2.00

et al., 1981). There is still some ambiguity as to the source of the reversible transition, which occurs at the lower temperature. Recently, we have studied the pH dependence of both the reversible and the irreversible transition temperatures using Fourier transform infrared (FT-IR) analysis of the amide I and amide II regions upon temperature increase (Heyes and El-Sayed, 2001). We found that the reversible transition temperature is the same (~80°C) for the native and samples regenerated with Ca^{2+} and Mg^{2+}. However, upon acidification into the acid blue membrane, the protein conformation is affected, the irreversible transition temperature reaches a low value of ~65°C, and no reversible transition is observed. It was postulated that the cation may be important for the protein structure and the observation of a reversible transition and that the protein thermal stability is strongly dependent on cation binding (Heyes and El-Sayed, 2001).

To investigate this further, we have extended the study to look at the transitions upon regenerating bR with a number of ions that have different properties. Mn^{2+} regenerated bR is used often in electron spin resonance (ESR) measurements and has been compared to Ca^{2+} binding (Dunach et al., 1987); hence we compare the Mn-BR and Ca-bR thermal transitions. We have also looked at the effect of regeneration of bR using Hg^{2+}, which is known not to regenerate the purple color or function of bR but has been found to bind competitively with Ca^{2+} (Ariki and Lanyi, 1986; Dunach et al., 1988). Also we have looked at a large divalent organic cation, which was found to regenerate the color and function (Tan et al., 1996; Fu et al., 1997). It was calculated that the organic cation may fit in the retinal cavity of the protein (Tan et al., 1996), provided it can reach the site, but it may not be able to force its way through the highly confined, hydrophobic space and orient itself to bind to this site upon addition to deionized bR.

MATERIALS AND METHODS

Bacteriorhodopsin (bR) was isolated and purified from *H. salinarum* by a standard procedure (Oesterhelt and Stoeckenius, 1974). The bR was deionized by passing through a column filled with ion-exchange resin (Bio-Rad AG-50W-X8, Bio-Rad Laboratories, Hercules, CA). Regeneration was performed by addition of chloride salt solution except for the organic cation for which the dibromide was used.

The organic cation was synthesized by a previously reported procedure (Menger and Wrenn, 1974; Tan et al., 1996). Briefly, 3.7 ml (0.032 mol) of 1,4-dibromo-butane in 8 ml of dry methanol was refluxed with 8.92 ml (0.064 mol) of triethylamine overnight to yield 3.5 g (0.0084 mol) of the product 1,4-bis(triethylammonium) butane dibromide, $C_{16}H_{38}Br_2N_2$. No further purification was necessary. Characterization by mass spectroscopy and ^1H NMR confirmed the desired product.

For the titration of the organic salt with deionized bR, the deionized bR solution was split into 10 equal amounts and placed in well washed plastic cuvettes to ensure no cation contamination. Microliter quantities of the cation solution were added to the cuvettes according to the desired molar ratios and allowed to equilibrate for at least 6 h. The visible absorption spectra were then measured on a Shimadzu (Kyoto, Japan) UV-3101PC UV-Vis spectrometer.

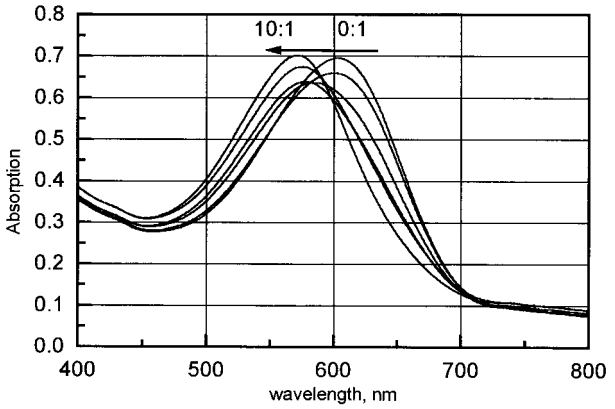

FIGURE 1 Visible absorption titration of Org-bR at ion:bR ratios of 0:1, 1:1, 2:1, 3:1, 4:1, and 10:1. The color shift for org-bR is similar to Ca-bR with an isosbestic point signaling equilibrium between the blue and purple species, which shifts to the purple with addition of the second cation.

For the FT-IR spectral measurements, all regenerated bR was made to an ion:bR ratio of 10:1 to be sure that complete regeneration has occurred (Zhang et al., 1992). The samples were then centrifuged to a pellet and placed in D_2O (99.9%, Sigma-Aldrich, Milwaukee, WI). This washing was repeated four to six times to ensure all available H_2O is exchanged for D_2O and labile amide N-H bonds are exchanged to N-D. The exact pH (pD) was measured before the final centrifugation and found to be between 6 and 7. The FT-IR spectra of the pellet in D_2O were then measured as previously described (Heyes and El-Sayed, 2001). All experiments are performed independently three to four times to ensure reproducibility and to determine errors in the observed transition temperatures.

RESULTS

Fig. 1 shows the visible absorption spectra of Org-bR regenerated from an ion:bR ratio of 0:1 to 10:1. The titration of the ion followed by UV-VIS spectroscopy is similar to that observed for Ca regeneration. There is little change until a 1:1 ion:bR ratio, then the λ_{max} begins to shift to the 568 nm of purple membrane with an isosbestic point consistent with the proposal that it is the second binding site that is responsible for controlling color as observed for other divalent cations.

The FT-IR spectra of M^{2+}-bR ($M^{2+} = Hg^{2+}$, Mn^{2+}, or the organic ion, Org^{2+}) measured from 20°C to 97°C are shown in Fig. 2, *A–C*. For each sample, as the temperature is raised there is a shift in the amide I peak from 1665 to 1652 cm^{-1} corresponding to the pre-melting transition, followed by an increase at 1623 cm^{-1} at the melting temperature. The amide II region of the spectrum shows decreasing N-H stretch intensity and increasing N-D intensity at 1545 cm^{-1} and 1439 cm^{-1}, respectively, with increasing temperature corresponding to the D_2O solvent accessing previously unexposed regions of the protein and exchanging with the labile amide N-H.

Differences in the spectra are seen more easily by using 20°C as the background and determining the changes in the spectra as the temperature is increased as shown in Fig. 3,

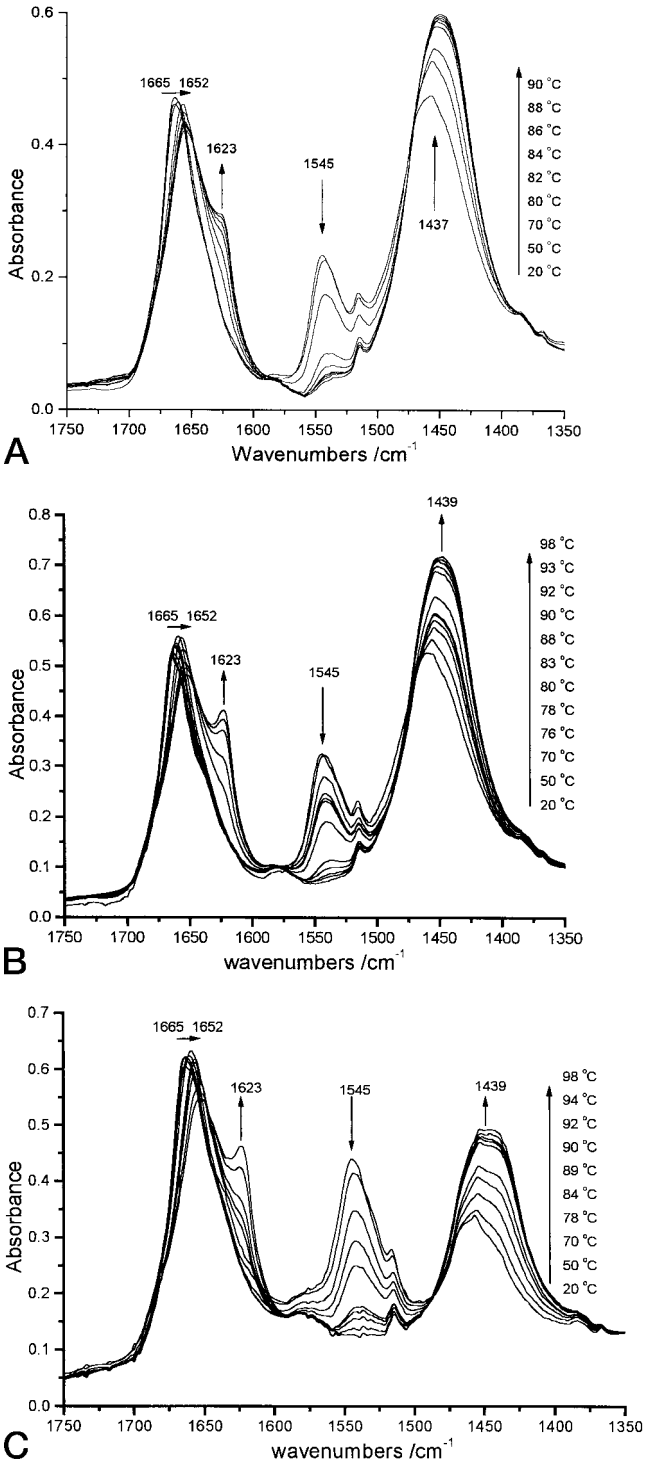

FIGURE 2 FT-IR spectra of Hg-bR (*A*), Mn-bR (*B*), and Org-bR (*C*), respectively, as temperature is raised from 20°C to melting. The reversible transition shifts the amide I region from 1665 cm^{-1} to 1652 cm^{-1}, which is followed at the melting transition by the increase in the shoulder at 1623 cm^{-1}, indicating uncoiling of the helices. There is a corresponding exchange of N-H with N-D with temperature, becoming more pronounced during the transitions.

A–C. For each regenerated bR there is little change in the amide I region of the spectra until the onset of the pre-melting transition at ~78–80°C. This is consistent with previous observations on the temperature dependence of the FT-IR spectrum of bR (Wang and El-Sayed, 1999; Heyes and El-Sayed, 2001). The 1665-cm^{-1} band begins to decrease, with a corresponding increase at 1652 cm^{-1}. Following this pre-melting transition, the 1623-cm^{-1} band begins to increase, signaling denaturation (melting) of the bR. The Hg-bR and the Mn-bR spectral changes compare well with the native and Ca-bR reported previously (Heyes and El-Sayed, 2001). The org-bR shows small but reproducible differences from the other M^{2+}-bR. There is still a shift at the pre-melting transition, but before melting (Fig. 2 *C* between 84°C and 90°C), the amide I band narrows from the high-frequency side, indicating a further change in the conformation in this temperature range. This is more easily seen in Fig. 3 *C*, where there are two peaks rising upon temperature increase, one at ~1653 cm^{-1} and another at ~1648 cm^{-1}. These rise at different temperatures (80°C and 88°C, respectively).

For all the samples there is some solvent exchange as the temperature is raised up to the pre-melting transition, as shown by the amide II regions in Fig. 3, *A–C*. This is an enthalpic process of the temperature dependence of the N-H to N-D exchange, because once the exchange has occurred it is irreversible due to $[D_2O] \gg [H_2O]$. The changes are more pronounced as the protein undergoes the conformational changes, thus exposing other parts of the protein to the D_2O.

To quantify the changes in the spectrum, the peak heights of the 1665-cm^{-1}, 1652-cm^{-1}, 1623-cm^{-1}, 1545-cm^{-1}, and 1439-cm^{-1} peaks are plotted as a function of temperature. This is shown in Fig. 4, *A–E*, with the derivatives of the curves shown as insets. The derivative allows one to determine the transition more accurately. Fig. 4 *B* shows the rise of the amide I band as the protein passes through its pre-melting transition, and the transition midpoint is determined from the derivative. The melting of the protein is similarly found from Fig. 4 *C*. The peak heights of each sample show similar temperature profiles. The 1652-cm^{-1} peak is independent of the cation used for the regeneration, but the 1623-cm^{-1} peak increases at different temperatures for each sample. Inspection of the peak intensities from the Fig. 4 *C* inset reveal that there are also two melting transitions for org-bR, suggesting a different melting mechanism for this cation than the metal cation regenerated bR samples.

These observations are summarized in Table 1. There is no variation in the pre-melting transition temperature (within the experimental error of 1–2°C) upon binding with cation. However, the irreversible denaturation temperature varies considerably with cation. Both Org^{2+} and Mn^{2+} have higher melting transition temperatures than the Ca^{2+} and Mg^{2+}, which are in turn higher than Hg^{2+}.

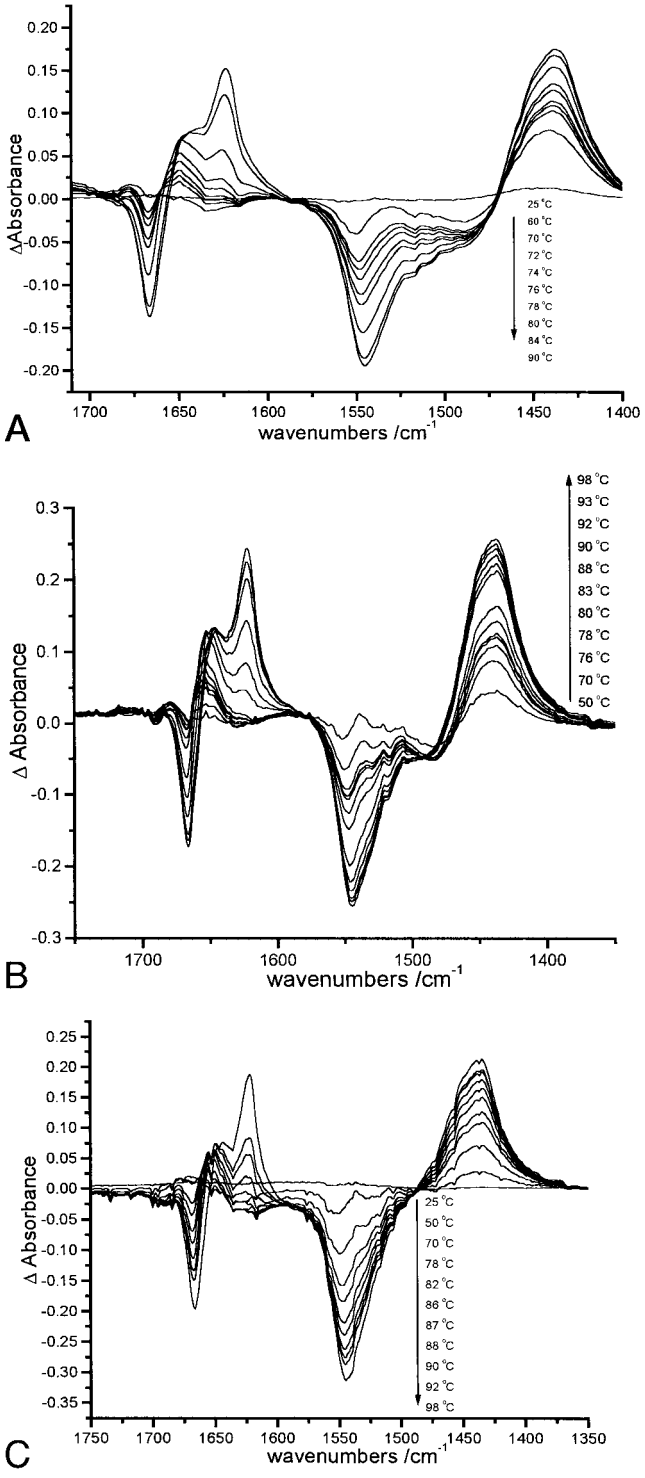

FIGURE 3 FT-IR difference of Hg-bR (*A*), Mn-bR (*B*), and Org-bR (*C*) using 20°C as baseline and subtracting from each of the higher temperatures. For the org-bR (*C*) one can see two species around 1652 cm^{-1} at higher temperature but only one for the metal ion regenerated bR. Each of these peaks are used to find ΔA of peaks for Fig. 4, *A–E*.

DISCUSSION

Effect of cations on protein structure

Upon binding to bR, a change in the conformation of the protein is observed. This was shown previously: as the native bR is acidified, the amide I band of the FT-IR spectrum changes to shows a lower, more usual α-helical stretching frequency of 1659 cm^{-1}, together with a larger degree of heterogeneity (Heyes and El-Sayed, 2001). A similar effect occurs in the FT-IR spectrum upon deionization at pH 4 (Masuda et al., 1995) and pH 5 (Dunach et al., 1989), which suggests that it is the cation and not the pH that is responsible for the conformation change, because native bR at pH 4.4 was shown to have the amide I band at 1665 cm^{-1} (Heyes and El-Sayed, 2001). Upon regeneration with Ca^{2+} or Mg^{2+}, it was shown that the amide I band is similar to the native (Heyes and El-Sayed, 2001). All the results presented here show a similar effect on the amide I band to Ca^{2+} and Mg^{2+} regeneration at physiological temperatures. Even bR regenerated with Hg^{2+} shows this amide I shift upon binding, even though it has been shown not to regenerate the purple color or the proton pumping function (Ariki and Lanyi, 1986). It has been shown that the Hg^{2+} does bind to bR (Dunach et al., 1988) and that some of the binding sites of Ca^{2+} regenerated bR are exchanged by Hg^{2+}, including the color-controlling site (Ariki and Lanyi, 1986). Ariki and Lanyi (1986) considered that the geometry of binding ligands around the ion might play a role in color regulation (Ariki and Lanyi, 1986). A recent titration of Ca^{2+} and Hg^{3+} cations with deionized bR by using in situ ATR-FTIR spectroscopy has shown global structural changes in the protein, lipids, and retinal isomeric configurations (Wang and El-Sayed, 2001). Our results show that the protein secondary conformation for deionized blue bR regenerated with any of the divalent ions considered in this and our previous study (Heyes and El-Sayed, 2001) are affected similarly to each other and to native bR at physiological temperature irrespective of their effect on retinal and on the functional significance. This indicates that the primary purpose of divalent cations is to mediate protein structure, and this is accomplished with any of the divalent cations that we have studied.

Effect of cations on thermal stability

The source of the pre-melting transition has not been unambiguously identified. Previous x-ray diffraction studies pointed to the transition as a breakdown of the hexagonal close-packed lattice of trimers that hold the bR in the two-dimensional crystal within the membrane, but where the bRs still have local order as trimers (Hiraki et al., 1981). Spectroscopic evidence, such as FT-IR (Rothschild and Clark, 1979b,a; Gibson and Cassim, 1989; Torres et al., 1995), Raman (Vogel and Gaertner, 1987), circular dichro-

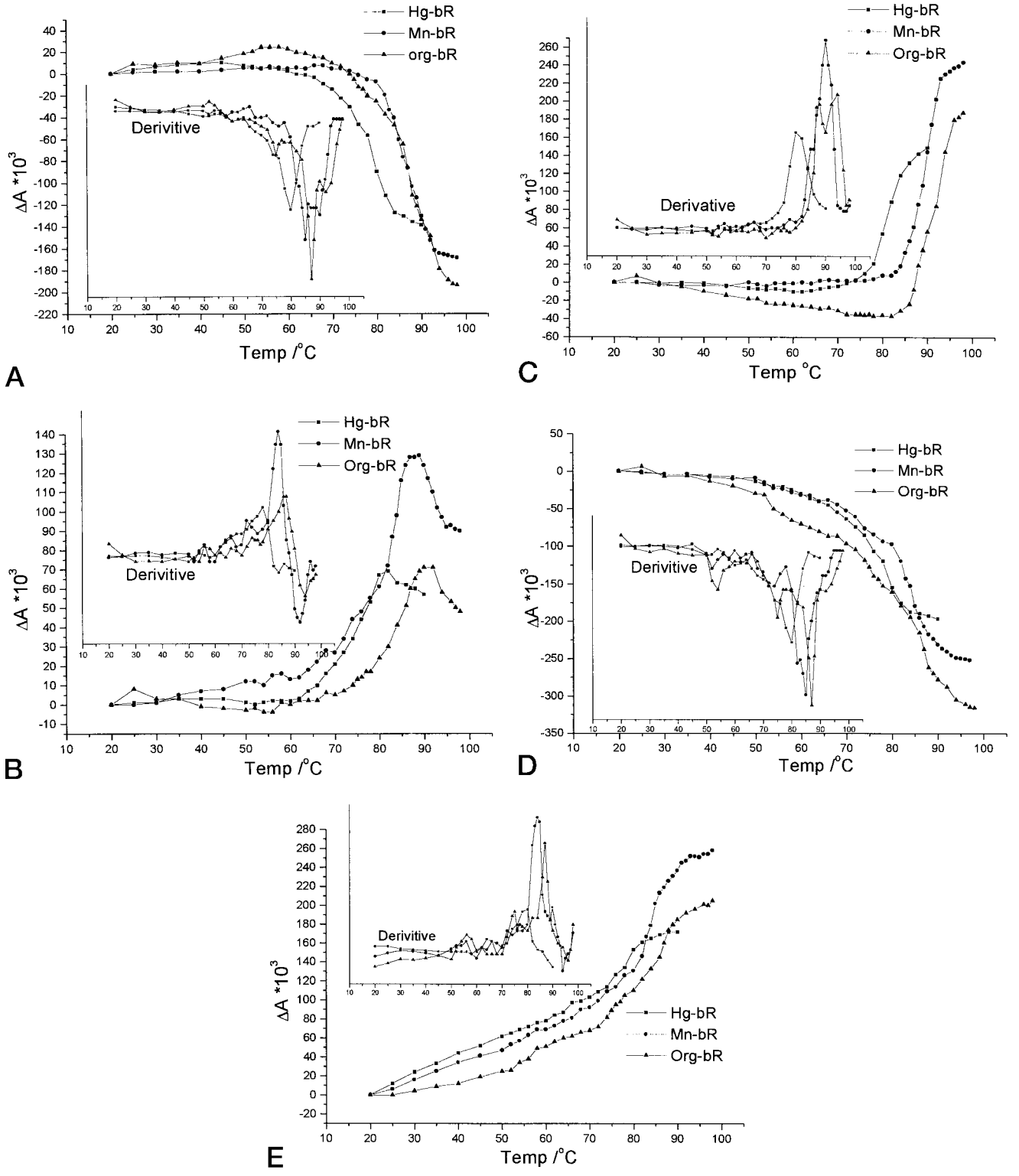

FIGURE 4 (*A–E*) Peak heights of 1665-cm^{-1}, 1652-cm^{-1}, 1623-cm^{-1}, 1545-cm^{-1}, and 1439-cm^{-1} bands for Hg-bR. These peaks correspond to the change in the amide I (*A–C*) and amide II (*D* and *E*) regions with temperature. There is little change in the amide I region until the pre-melting transition at ~80°C. Then the 1665-cm^{-1} peak decreases with an increase in the 1652-cm^{-1} band. The 1623-cm^{-1} band signals the melting transition. The insets of these figures are the first derivatives of the curves in which one can determine the transition midpoint more accurately; *B* is used to determine the pre-melting transition and *C* the melting transition. The N-H to N-D exchange can be followed from *D* and *E*, respectively. It is shown that upon heating and especially during the transitions, more parts of the protein become exposed to the D_2O solvent, and proton for deuteron exchange occurs.

TABLE 1 Transition temperatures of Ca-bR, Mg-bR, Mn-bR, Hg-bR, and Org-bR

Native	Pre-melting transition	Melting transition
Native*	78 ± 2°C	97 ± 1°C
Ca-bR*	78 ± 2°C	84 ± 2°C
Mg-bR*	78 ± 2°C	82 ± 2°C
Hg-bR	78 ± 1°C	80 ± 1°C
Mn-bR	78 ± 1°C	88 ± 1°C
Org-bR	80 ± 2°C	91 ± 1°C

*From Heyes and El-Sayed (2001).

ism (Gibson and Cassim, 1989), linear dichroism (Torres et al., 1995), and ^{13}C NMR (Tuzi et al., 1994; Tuzi et al., 1996; Kawase et al., 2000), has pointed to the possibility of an α_{II}-helix in native bR, where the ϕ and ψ angles differ from the normal α_I-helix by $+26^o$ and $-20°$, respectively, resulting in lengthening of the intrahelical H-bond length by 0.14 Å and a 10-cm^{-1} increase in the FT-IR amide I stretching frequency from the usual 1652 cm^{-1} to 1663 cm^{-1} (Krimm and Dwivedi, 1982). The fact that the amide I FT-IR band of bR shifts from 1663 cm^{-1} toward 1652 cm^{-1} during this pre-melting transition indicates that the α-helix may change between these two conformations during the pre-melting transition. It is plausible that these two effects are coupled and that the α conformation allows the lattice to be formed or vice versa. Whether only one of these explanations or both are correct for the observed FT-IR shift, it is reasonable to discuss the cations in terms of their effect on the temperature of the transitions.

The pre-melting transition is observed for all samples regenerated with divalent cations and occurs at the same 80°C temperature (within the experimental error). However, if no ions are present, as is the case with acid blue, no transition is observed. This indicates that a cation is necessary to induce the conformation change that leads to the 1665-cm^{-1} frequency. Once the temperature is raised to 80°C, the conformation shifts to as if there was no ion present independent of which ion was bound. Cladera et al. (1988) did not observe the pre-melting transition for Hg-bR using calorimetry. This is most probably due to the closeness in temperature of the pre-melting transition and the melting transition causing an overlap in the differential scanning calorimetry profiles. They do see the melting begin at 77°C, lower than our results by 3–4°C, which may be the onset of the pre-melting transition peak convoluting with the melting transition peak. Whatever the source of the amide I shift, breakdown of the lattice or the α_{II} to α_I conformation change or both, the pre-melting transition seems not to be affected by any possible differences in binding of ions in the native or regenerated bR as has been observed for example in Ca^{2+} and Mn^{2+} (Jonas and Ebrey, 1991; Ariki and Lanyi, 1986; Zhang et al., 1992; Dunach et al., 1987). This indicates that once the divalent ions are present in bR, the thermodynamics of this transition are independent of other factors such as position of the binding sites, binding strengths, or ion size.

All cation-regenerated samples have the irreversible melting temperature higher than the deionized bR but lower than the native bR. Furthermore, all the regenerated bR samples have the melting transition higher than 80°C, where the pre-melting transition occurs. The actual melting temperature varies from sample to sample and can vary by as much as 10°C between Hg-bR and Org-bR. This strong dependence on cation can be explained only by the cation interacting with the protein differently depending on its identity. Whereas the pre-melting transition seems to be an intrinsic property of the protein, provided ions are bound somewhere, the melting is a property of both the protein and the cation. Hg^{2+} offers the least protection to melting but still more than no ion present. Ca^{2+} and Mg^{2+} offer some protection and the Mn^{2+} and Org^{2+} offer the highest protection to unfolding. Hg^{2+} has been shown to bind competitively with Ca^{2+} to bR but binds with different geometry (linear versus octahedral) (Ariki and Lanyi, 1986). The geometry may also explain the differences in melting temperature by lower binding coordination. The higher melting temperatures of Mn^{2+} and Org^{2+} are unexpected and may be explained by different binding sites and mechanisms, which will be discussed below.

The irreversible denaturation of bR is accompanied by an increase in the intensity of the band at 1623 cm^{-1}. This increase stops when the ratio of α-helix to random coil approaches 40% as estimated from Fig. 2, *A–C*. Upon cooling after denaturation, there is very little change in this ratio (not shown), even though the bands do broaden slightly. Thus, from Fig. 2 it is estimated that less than one-half of the protein helices unwind into random coils. Hence, even the melted protein contains some helical domains in the normal α_I conformation. It is not known exactly which parts of the protein have unwound, but upon melting, the retinal loses its characteristic opsin-shifted λ_{max} and absorbs at the usual 420 nm of unbound retinal Schiff base (Hiraki et al., 1981). This indicates that the Schiff base has been exposed to water and becomes hydrolyzed.

The question remains whether the ions are still present in the protein and thus whether they are responsible for holding the unfolded helices together. If the model of α_I and α_{II} helices being present in bR at physiological temperatures is considered, then it is possible that during the pre-melting transition, part of the protein held in the α_{II} conformation by the cation is transformed into α_I, and then some domains begin to unwind during the denaturation (melting) transition. If ions are still bound to the protein, then it is possible that the unwinding process would occur in the parts of the protein not bound to the ion due to the extra stabilizing tertiary forces from the cation. This would obviously depend on the binding sites and strengths of the ion, and differences observed in the melting can be used to infer possible differences in the binding. Whatever the differ-

ences in binding, the fact that differences are observed in the melting temperatures and mechanisms suggests that interactions with the protein are different and contradict random binding and pH mediation from the surface being the only binding. If the binding were random, and pH mediated only by presence of the number of cations at the membrane surface, then the melting temperatures should depend only on the differences in ionic strength of ions added. Because all samples were regenerated with a 10:1 molar ratio of ion:bR and excess ions washed in D_2O, then differences in ionic strengths are negligible and no ion dependence on melting should have been observed. This argument is consistent with the Hg^{2+} studies by Ariki and Lanyi (1986) and Dunach et al. (1988), where, had binding been confined to the double layer, then Hg^{2+} should regenerate the purple functional form in the same way as other divalent ions. Varo et al. (1999) later covalently linked a dye to the protein at engineered cysteine residues to measure surface pH as Ca^{2+} is added to deionized bR. From the observed correlation between the surface and measured pH, they concluded that binding is nonspecific to the surface. Eliash et al. (2001) as well as Tuzi et al. (1999) have found specific exposed binding sites near the surface that could also affect surface pH.

Binding sites of the different cations to bbR

One must consider the fact that upon removal of the native ions, the protein changes conformation considerably (Heyes and El-Sayed, 2001) and may even lose the hexagonal packing (Heyn et al., 1989) (later postulated to be a result of partial dehydration (Wakatsuki et al., 1994)), and upon regeneration it seems unlikely that all binding sites are intact. Conclusions drawn from binding to deionized bR may not hold for native grown bR, where the ions are present as the protein grows from the start and the protein may fold around the ion as it grows. Thus, color and secondary structure of native bR may be mediated differently than for regenerated bR but give the same final observations, i.e., purple color and higher amide I frequency. This could also help to explain the lower melting temperature for regenerated bR than for native bR and the dependence on the cation identity and pH.

It has been postulated that a small metal cation such as Ca^{2+} would fit in a cavity close to the retinal Schiff base, countered by Asp85, Asp212, Tyr57, Tyr185, and Arg82 (Jonas and Ebrey, 1991). Removal of retinal eliminates one of these sites for Ca^{2+} (Yang and El-Sayed, 1995), and the binding affinities for Ca^{2+} are reduced significantly when the charged residues, Asp-85, Asp-212, Arg-82, and the H-bonding residue, Tyr-185, are mutated to neutral residues and the affinity for the second site for Tyr-185 is reduced more than the first site (Zhang et al., 1993). These previous studies have suggested that Ca^{2+} binding to deionized bR occurs at two sites that are internal to the protein and at least one that is close to the retinal. A number of other studies have found that only the second high-affinity binding site affects the color of the chromophore (Ariki and Lanyi, 1986; Zhang et al., 1992, 1993; Masuda et al., 1995)

Recent experiments have also brought about the possibility of binding sites at other, more exposed sites within the protein. Tuzi et al. (1999) used ^{13}C NMR spectroscopy to deduce a Ca^{2+} binding site in the F-G loop of bR, whereas Eliash et al. (2001) have used ESR spectroscopy to show a Mn^{2+}-specific binding site on the extracellular side. An older ESR study found 5 Mn^{2+} binding sites with fairly high affinities (Dunach et al., 1987). It was also postulated that the titration of Asp85 and the color-controlling site are not coupled (Fu et al., 1997; Eliash et al., 1999). The differences observed in the high-affinity sites for Ca^{2+} and Mn^{2+} suggest that their binding to bR are not identical, and may regulate the color differently. Ca^{2+} effect may be more direct and short range than Mn^{2+}. The differences in the melting temperatures observed seem to offer additional evidence to this. The larger concentration of Mn^{2+} toward the surface offers a greater shielding effect to uncoiling and solvent penetration into the protein, whereas the Ca^{2+} does not offer as much shielding but still more than deionized bR or Hg^{2+} regenerated bR. As mentioned earlier, the geometry differences may explain the differences in color regulation and lower thermal stability for the Hg^{2+} due to even lower shielding than the Ca^{2+}. Mg^{2+} has been previously shown to bind similarly to Ca^{2+} (Yoo et al., 1995; Griffiths et al., 1996b), and our results on the similar melting temperatures agree with this.

The organic cation, due to its large size, is unlikely to travel through the protein to bind close to the retinal, even though a possible binding site has been proposed (Tan et al., 1996). However, the melting transition occurs at a higher temperature than the metal cation regenerated bR. The results for the FT-IR spectral changes upon denaturation of the Org-bR differ from the metal cation regenerated bR. This suggests that the binding of the organic cation is different from that of the metal cation in such a way as to affect the mechanism of melting. Both Mn-bR and Org-bR each have rather high melting temperatures, suggesting that tertiary interaction strengths present are similar for these two. However, the shape of the amide I band upon melting is different for each of them, suggesting that binding to the helices is different. The spacing between the two charges on the organic ion may be responsible for this. It could be acting effectively as an anchor between helices and increasing the resistance to uncoiling even more than the Mn^{2+} and resulting in a two-stage melting where binding of part of the Org^{2+} may still be intact during the first stages of the melting process. Also, the two separated charges on the organic cation could affect the pre-melting process giving rise to two resolved bands around 1650 cm^{-1} instead of one.

The titration effect on the color of the Org-bR is the same as for metal ion binding, except for Hg^{2+}. Obviously, the

protein is a much larger part of the system than the retinal site, and pinpointing the domains of the cation effects are difficult. It seems clear that the environment around the retinal may be affected from further away than the immediate vicinity and that the geometry plays an important role in the retinal and the protein stability. Thus, even though we cannot conclude that the binding sites are close to the retinal in native bR or bR regenerated with cations, we can conclude that the ions interact with the protein differently depending on size and geometry but that they do interact directly with the protein. This interaction is strong and direct enough to have a rather large effect on both the secondary and tertiary structures, maybe causing electronic effects on the retinal by different means. If there is direct protein interaction, then this must be specific, because random sites are in the bilayer only as explained by the Guoy-Chapman theory. It is possible that color is regulated by the cation binding to specific sites in the protein and holding it in a particular conformation from exposed areas of the protein or from inside, depending on the cation, and both the protein conformation and the cation geometry regulates the retinal and Asp-85. That is not to say that these specific interactions are the same for all ions; indeed, this is unlikely, but it is not possible at this point to say whether the differences lie in different sites or within the same sites. In all cases, however, the thermodynamic constraints that the ion has on the protein structure lower than 80°C are removed above this temperature, because all samples take up the usual α-helical 1652-cm^{-1} conformation, but tertiary constraints are not. It seems clear that native and regenerated bR do not have all the same binding sites and/or strengths, and binding constants calculated from regeneration studies might not accurately give those for native bR.

This work was supported by the Chemical Sciences, Geosciences, and Biosciences Division, Office of Basic Energy Science, Office of Sciences, U.S. Department of Energy (under grant DE-FG02–97ER14799).

REFERENCES

Ariki, M., and J. K. Lanyi. 1986. Characterization of metal ion-binding sites in bacteriorhodopsin. *J. Biol. Chem.* 261:8167–8174.

Birge, R. R., N. B. Gillespie, E. W. Izaguirre, et al. 1999. Biomolecular electronics: protein-based associative processors and volumetric memories. *J. Phys. Chem. B.* 103:10746–10766.

Brouillette, C. G., D. D. Muccio, and T. K. Finney. 1987. pH dependence of bacteriorhodopsin thermal unfolding. *Biochemistry.* 26:7431–7438.

Chang, C. H., J. G. Chen, R. Govindjee, and T. Ebrey. 1985. Cation binding by bacteriorhodopsin. *Proc. Natl. Acad. Sci. U.S.A.* 82: 396–400.

Chronister, E. L., T. C. Corcoran, L. Song, and M. A. El-Sayed. 1986. On the molecular mechanisms of the Schiff base deprotonation during the bacteriorhodopsin photocycle. *Proc. Natl. Acad. Sci. U.S.A.* 83: 8580–8584.

Cladera, J., M. L. Galisteo, M. Dunach, P. L. Mateo, and E. Padros. 1988. Thermal denaturation of deionized and native purple membranes. *Biochim. Biophys. Acta.* 943:148–156.

Drachev, L. A., A. D. Kaulen, and L. V. Khitrina. 1988. Polyvalent metal salts as inhibitors of photochemical conversions of bacteriorhodopsin. *Biokhimiya.* 53:663–667.

Dunach, M., E. Padros, A. Muga, and J. L. R. Arrondo. 1989. Fourier-transform infrared studies on cation binding to native and modified purple membranes. *Biochemistry.* 28:8940–8945.

Dunach, M., M. Seigneuret, J. L. Rigaud, and E. Padros. 1987. Characterization of the cation binding sites of the purple membrane. Electron spin resonance and flash photolysis studies. *Biochemistry.* 26:1179–1186.

Dunach, M., M. Seigneuret, J. L. Rigaud, and E. Padros. 1988. Influence of cations on the blue to purple transition of bacteriorhodopsin. Comparison of calcium and mercury(2+) binding and their effect on the surface potential. *J. Biol. Chem.* 263:17378–17384.

Ebrey, T. G. 1993. Light energy transduction in bacteriorhodopsin. *In* Thermodynamics of Membrane Receptor Channels. M. B. Jackson, editor. CRC Press, Boca Raton, FL. 353–387.

Eliash, T., M. Ottolenghi, and M. Sheves. 1999. The titrations of Asp-85 and of the cation binding residues in bacteriorhodopsin are not coupled. *FEBS Lett.* 447:307–310.

Eliash, T., L. Weiner, M. Ottolenghi, and M. Sheves. 2001. Specific binding sites for cations in bacteriorhodopsin. *Biophys. J.* 81: 1163–1170.

El-Sayed, M. A., D. Yang, S.-K. Yoo, and N. Zhang. 1995. The effect of different metal cation binding on the proton pumping in bacteriorhodopsin. *Isr. J. Chem.* 35:465–474.

Fu, X., S. Bressler, M. Ottolenghi, T. Eliash, N. Friedman, and M. Sheves. 1997. Titration kinetics of Asp-85 in bacteriorhodopsin: exclusion of the retinal pocket as the color-controlling cation binding site. *FEBS Lett.* 416:167–170.

Gibson, N. J., and J. Y. Cassim. 1989. Evidence for an alpha II-type helical conformation for bacteriorhodopsin in the purple membrane. *Biochemistry.* 28:2134–2139.

Griffiths, J. A., M. A. El-Sayed, and M. Capel. 1996a. Effect of binding of lanthanide ions on the bacteriorhodopsin hexagonal structure: an x-ray study. *J. Phys. Chem.* 100:12002–12007.

Griffiths, J. A., J. King, R. Browner, and M. A. El-Sayed. 1996b. Calcium and magnesium binding in native and structurally perturbed purple membrane. *J. Phys. Chem.* 100:929–933.

Hampp, N. 2000. Bacteriorhodopsin as a photochromic retinal protein for optical memories. *Chem. Rev.* 100:1755–1776.

Heyes, C. D., and M. A. El-Sayed. 2001. The effect of temperature, pH and metal ion binding on the secondary structure of bacteriorhodopsin: FT-IR study of the melting and pre-melting transition temperatures. *Biochemistry.* 40:11819–11827.

Heyn, M. P., C. Dudda, H. Otto, F. Seiff, and I. Wallat. 1989. The purple to blue transition of bacteriorhodopsin is accompanied by a loss of the hexagonal lattice and a conformational change. *Biochemistry.* 28: 9166–9172.

Hiraki, K., T. Hamanaka, T. Mitsui, and Y. Kito. 1981. Phase transitions of the purple membrane and the brown holo-membrane: x-ray diffraction, circular dichroism spectrum and absorption spectrum studies. *Biochim. Biophys. Acta.* 647:18–28.

Jackson, M. B., and J. M. Sturtevant. 1978. Phase transitions of the purple membranes of *Halobacterium halobium*. *Biochemistry.* 17:911–915.

Jang, D. J., T. C. Corcoran, and M. A. El-Sayed. 1988. Effects of metal cations, retinal, and the photocycle on the tryptophan emission in bacteriorhodopsin. *Photochem. Photobiol.* 48:209–217.

Jonas, R., and T. G. Ebrey. 1991. Binding of a single divalent cation directly correlates with the blue-to-purple transition in bacteriorhodopsin. *Proc. Natl. Acad. Sci. U.S.A.* 88:149–153.

Kawase, Y., M. Tanio, A. Kira, S. Yamaguchi, S. Tuzi, A. Naito, M. Kataoka, J. K. Lanyi, R. Needleman, and A. Saito. 2000. Alteration of conformation and dynamics of bacteriorhodopsin induced by protonation of Asp85 and deprotonation of Schiff base as studied by ^{13}C-NMR. *Biochemistry.* 39:14472–14480.

Kimura, Y., A. Ikegami, and W. Stoeckenius. 1984. Salt and pH-dependent changes of the purple membrane absorption spectrum. *Photochem. Photobiol.* 40:641–646.

Kresheck, G. C., C. T. Lin, L. N. Williamson, W. R. Mason, D. J. Jang, and M. A. El-Sayed. 1990. The thermal stability of native, delipidated, deionized and regenerated bacteriorhodopsin. *J. Photochem. Photobiol. B.* 7:289–302.

Krimm, S., and A. M. Dwivedi. 1982. Infrared spectrum of the purple membrane: clue to a proton conduction mechanism. *Science.* 216: 407–408.

Lanyi, J. K. 1995. Bacteriorhodopsin as a model for proton pumps. *Nature.* 375:461–463.

Leuke, H., B. Schobert, H. T. Richter, J. P. Cartailler, and J. K. Lanyi. 1999. Structure of bacterierhodopsin at 1.55 Angstron resolution. *J. Mol Biol.* 291:899–911.

Masuda, S., M. Nara, M. Tasumi, M. A. El-Sayed, and J. K. Lanyi. 1995. Fourier transform infrared spectroscopic studies of the effect of Ca^{2+} binding on the states of aspartic acid side chains in bacteriorhodopsin. *J. Phys. Chem.* 99:7776–7781.

Mathies, R. A., S. W. Lin, J. B. Ames, and W. T. Pollard. 1991. From femtoseconds to biology: mechanism of bacteriorhodopsin's light-driven proton pump. *Annu. Rev. Biophys. Biophys. Chem.* 20:491–518.

Menger, F. M., and S. Wrenn. 1974. Interfacial and micellar properties of bolaform electrolytes. *J. Phys. Chem.* 78:1387–1390.

Mowery, P. C., R. H. Lozier, Q. Chae, Y.-W. Tseng, M. Taylor, and W. Stoeckenius. 1979. Effect of acid pH on the absorption spectra and photoreactions of bacteriorhodopsin. *Biochemistry.* 18:4100–4107.

Oesterhelt, D., and W. Stoeckenius. 1974. Isolation of the cell membrane of *Halobacterium halobium* and its fractionation into red and purple membrane. *Methods Enzymol.* 31:667–678.

Rothschild, K. J., and N. A. Clark. 1979a. Anomalous amide I infrared absorption of purple membrane. *Science.* 204:311–312.

Rothschild, K. J., and N. A. Clark. 1979b. Polarized infrared spectroscopy of oriented purple membrane. *Biophys. J.* 25:473–487.

Stoeckenius, W., R. H. Lozier, and R. A. Bogomolni. 1979. Bacteriorhodopsin and the purple membrane of halobacteria. *Biochim. Biophys. Acta.* 505:215–278.

Szundi, I., and W. Stoeckenius. 1987. Effect of lipid surface charges on the purple-to-blue transition of bacteriorhodopsin. *Proc. Natl. Acad. Sci. U.S.A.* 84:3681–3684.

Szundi, I., and W. Stoeckenius. 1988. Purple-to-blue transition of bacteriorhodopsin in a neutral lipid environment. *Biophys. J.* 54:227–232.

Szundi, I., and W. Stoeckenius. 1989. Surface pH controls purple-to-blue transition of bacteriorhodopsin: a theoretical model of purple membrane surface. *Biophys. J.* 56:369–383.

Tan, E. H. L., D. S. K. Govender, and R. R. Birge. 1996. Large organic cations can replace Mg^{2+} and Ca^{2+} ions in bacteriorhodopsin and maintain proton pumping ability. *J. Am. Chem. Soc.* 118:2752–2753.

Torres, J., F. Sepulcre, and E. Padros. 1995. Conformational changes in bacteriorhodopsin associated with protein-protein interactions: a functional alpha I-alpha.II helix switch? *Biochemistry.* 34:16320–16326.

Tuzi, S., A. Naito, and H. Saito. 1994. ^{13}C NMR study on conformation and dynamics of the transmembrane alpha-helixes, loops, and C-terminus of [3–13C]Ala-labeled bacteriorhodopsin. *Biochemistry.* 33: 15046–15052.

Tuzi, S., A. Naito, and H. Saito. 1996. Temperature-dependent conformational change of bacteriorhodopsin as studied by solid-state ^{13}C NMR. *Eur. J. Biochem.* 239:294–301.

Tuzi, S., S. Yamaguchi, M. Tanio, H. Konishi, S. Inoue, A. Naito, R. Needleman, J. K. Lanyi, and H. Saito. 1999. Location of a cation binding site in the loop between helices F and G of bacteriorhodopsin as studied by 13-C NMR.

Varo, G., L. S. Brown, R. Needleman, and J. K. Lanyi. 1999. Binding of calcium ions to bacteriorhodopsin. *Biophys. J.* 76:3219–3226.

Vogel, H., and W. Gaertner. 1987. The secondary structure of bacteriorhodopsin determined by Raman and circular dichroism spectroscopy. *J. Biol. Chem.* 262:11464–11469.

Wakatsuki, S., Y. Kimura, W. Stoeckenius, N. Gillis, D. Eliezer, K. O. Hodgson, and S. Doniach. 1994. Blue form of bacteriorhodopsin and its order-disorder transition during dehydration. *Biochim. Biophys. Acta.* 1185:160–166.

Wang, J., and M. A. El-Sayed. 1999. Temperature jump induced secondary structural change of the membrane protein bacteriorhodopsin in the premelting temperature region: a nanosecond time-resolved Fourier transform infrared study. *Biophys. J.* 76:2777–2783.

Wang, J., and M. A. El-Sayed. 2001. The effect of metal cation binding on the protein, lipid and retinal isomeric ratio in regenerated bacteriorhodopsin of purple membrane. *Photochem. Photobiol.* 73:564–571.

Yang, D., and M. A. El-Sayed. 1995. The Ca^{2+} binding to deionized monomerized and to retinal removed bacteriorhodopsin. *Biophys. J.* 69:2056–2059.

Yoo, S.-K., E. S. Awad, and M. A. El-Sayed. 1995. Comparison between the binding of Ca^{2+} and Mg^{2+} to the two high-affinity sites of bacteriorhodopsin. *J. Phys. Chem.* 99:11600–11604.

Zhang, Y. N., M. A. El-Sayed, M. L. Bonet, J. K. Lanyi, M. Chang, B. Ni, and R. Needleman. 1993. Effects of genetic replacements of charged and hydrogen-bonding residues in the retinal pocket on calcium binding to deionized bacteriorhodopsin. *Proc. Natl. Acad. Sci. U.S.A.* 90: 1445–1449.

Zhang, Y. N., L. L. Sweetman, E. S. Awad, and M. A. El-Sayed. 1992. Nature of the individual calcium binding sites in Ca^{2+}-regenerated bacteriorhodopsin. *Biophys. J.* 61:1201–1206.